

IMPLEMENTATION AND OPERATION OF ELECTRON CLOUD DIAGNOSTICS FOR CESRTA*

Y. Li[#], X. Liu, V. Medjidzade, J. Conway, M. Palmer
CLASSE, Cornell University, Ithaca, NY 14853, U.S.A.

Abstract

The vacuum system of Cornell Electron Storage Ring (CESR) was successfully reconfigured to support CesrTA physics programs, including electron cloud (EC) build-up and suppression studies. One of key features of the reconfigured CESR vacuum system is the flexibility for exchange of various vacuum chambers with minimized impact to the accelerator operations. This is achieved by creation of three short gate-valve isolated vacuum sections. Over the last three years, many vacuum chambers with various EC diagnostics (such as RFAs, shielded pickups, etc) were rotated through these short experimental sections. With these instrumented test chambers, EC build-up was studied in many magnetic field types, including dipoles, quadrupoles, wigglers and field-free drifts. EC suppression techniques by coating (TiN, NEG and a-C), surface textures (grooves) and clearing electrode are incorporated in these test chambers to evaluate their vacuum performance and EC suppression effectiveness. We present the implementation and operations of EC diagnostics.

INTRODUCTION

With the successful reconfiguration of Cornell Electron Storage Ring (CESR) [1], CesrTA provides unique opportunities for study electron cloud growth and mitigation, and ultra-low emittance lattice development and tuning, as well as beam instrumentation R&D, that are critical for the global design efforts of the International Linear Collider Damping Rings. As depicted in Fig 1, two long straight experimental sections and two very short experimental sections were created to provide flexibility of the CesrTA studies, to continue to support X-ray users at CHESS (Cornell High-Energy Synchrotron Sources). These experimental sections may be isolated via gate valves, so that test chambers could be exchanged without significantly impact overall accelerator operations. In these experimental sections, many new vacuum chambers were deployed with various EC diagnostics, such as retarding field analyzers (RFAs) for measuring steady-state EC build-up [2], RF shielded pickups [3] for studying EC growth, and TE wave transducer/receiver beam buttons [4]. With these EC diagnostics, effectiveness of many types of EC

suppression techniques was evaluated in the test chambers. The details of these EC diagnostics and the corresponding measurements are described in separated papers in these proceeding. This paper is focussed on vacuum aspects of the implementation and the operational performances of these diagnostics and test chambers.

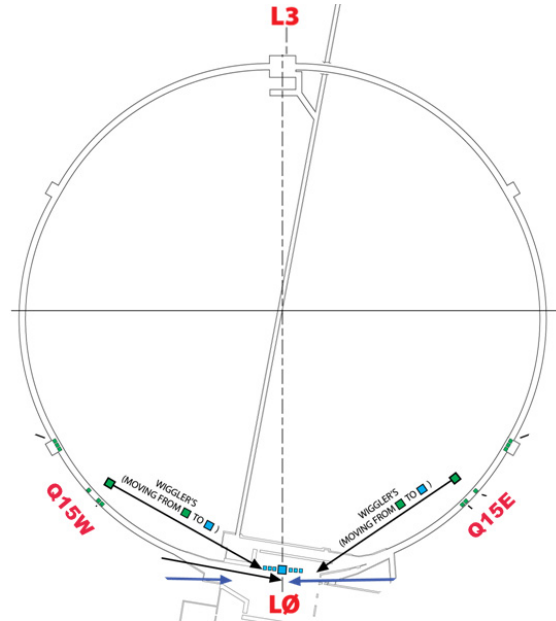


Figure 1: Four experimental sections were created after re-configuration of CESR vacuum system, including two long straights in south IR (L0), the north IR (L3) and two short sections in the arcs (namely, Q15W and Q15E). These sections may be isolated by gate valves to allow flexibility in deployments of various test chambers.

SOUTH IR EXPERIMENTAL SECTION

After removal of the center CLEO HEP Detector package, the South IR experimental section (~17.6 m in length), as shown in Fig 2, hosts a string of six superconducting wigglers (SCWs). The three SCWs in the West of L0 were fitted beampipes equipped with the thin-style RFAs [5]. A total of four RFA SCWs were constructed and rotated through this experimental section. The four RFA SCWs have different beampipe interior features, and they are (1) bare copper, (2) copper with TiN coating, (3) copper with a copper grooved bottom plate (which was later coated with TiN), and (4) copper with a EC clearing electrode at the bottom.

* Work supported by the US National Science Foundation (PHY- 0734867), the US Department of Energy (DE-FC02-08ER41538), and the Japan / US Cooperation Program

YL67@Cornell.edu

RFA SCW with a grooved plate

Fig 3 shows the structure of the RFA SCW with a Cu-groove plate, and details of the grooves. Simulations [6] showed that in order to suppress secondary electron emission yield (SEY), the tips and valleys of the

triangular grooves must be very sharp, with radius less than 0.1mm. The required sharpness was achieved via a special milling process. The groove plate is e-beam welded to the bottom of the RFA SCW beampipe.

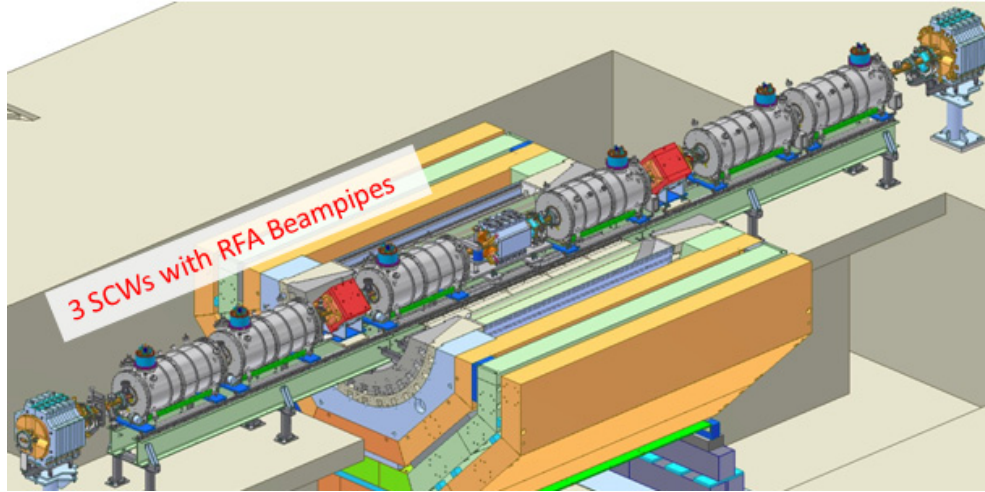


Figure 2: CESR South IR straight section with six super-conduction wiggler magnets (SCWs). Three of these SCWs in the west side are fitted with RFA-instrumented beampipe. Various mitigation techniques, including TiN coating, grooved beampipe and clearing electrode, were tested with these three SCWs

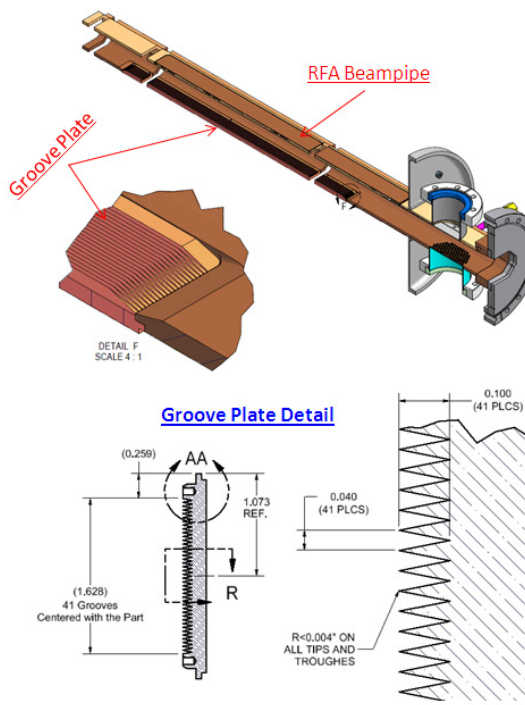


Figure 3: RFA SCW beampipe with a copper grooved plate. The groove plate has 41 triangular grooves of 1-mm spacing, and is integrated to the bottom beampipe via E-beam weld.

The grooved RFA SCW was installed in the South IR section between July 2009 and March 2010 for CesarTA experiment runs. After the 2009-2010 CesarTA experiment

runs and CHESS high current runs, the grooved assembly was removed from CESR during an accelerator shutdown in March 2010. A careful optical close-up inspection was performed on the groove plate over its entire length, and the inspection did not detect any beam-induced damage to the groove tips.

TiN coating was then applied to the interior surfaces of the grooved beampipe, via DC sputtering process. With careful arrangement of multiple titanium electrodes, a uniform TiN coating (~0.5μm in thickness) was deposited onto the grooves without visible shadowing. The TiN coated RFA SCW assembly was re-installed in the west South IR for further CesarTA experiments.

RFA SCW with Clearing Electrode

An electron cloud clearing electrode is deployed on one of the RFA SCW. The clearing electrode is based on the KEK design [7], using thermal spray thin film technique. As illustrated in Fig.4, the electrode is formed by a 0.2-mm thick alumina base film and a 0.2-mm thick tungsten film. DC voltage up to 1.5 kV can be applied to the electrode through an N-type vacuum feedthrough and a low profile contact button. This clearing electrode has very low higher-order-mode loss (HOML), which is critical for both the CesarTA and the CHESS operations. This RFA SCW was installed in the South IR region in March 2010, and has successfully operated through two CesarTA experiment runs and the CHESS X-ray runs. A thermocouple was attached immediately underneath the electrode, near the contact button. No measurable beam induced heating was detected with stored total beam current as high as 430mA. A close-up inspection during

January 2011 shutdown found that the electrode and the electric contact are in excellent condition.

Vacuum Performance

The South IR section is pumped by six non-evaporable getter (NEG) pumps (as primary pumps) and six small ion pumps (for non-gettable gases). Vacuum performance of this section is monitored by six evenly spaced cold-cathode ion gauges (CCGs) and a residual gas analyzer (RGA) at center of the section.

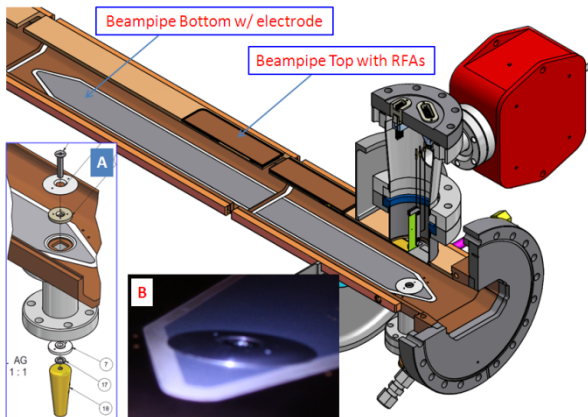


Figure 4: RFA SCW beampipe with a clearing electrode. The electrode was deposited onto the bottom half of the beampipe via thermal-spray technique. Insert A illustrates structure of low-profile electric contact, and insert B is a image of the contact button taken during post operation inspection in January 2011.

The beam processing of the vacuum chambers is monitored during CHESS X-ray runs, where the conditions for the stored beams are constant and stable. The measure synchrotron radiation (SR) induced pressure rises at three CCGs are plotted in Fig. 5 as a function of total beam dose. During the CHESS runs, the east side and the west side of the section receive comparable SR flux. However, the west sides had much higher SR-induced outgassing. One plausible source of higher outgassing rate in west side is due to the TiN coating..

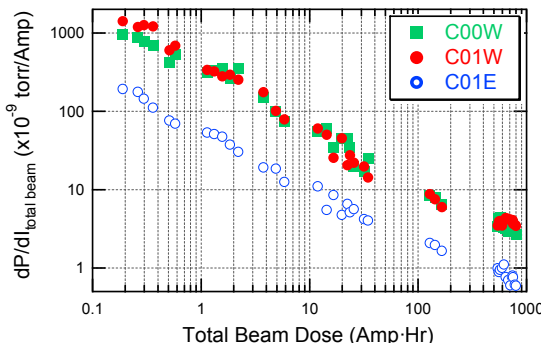


Figure 5: Beam conditioning of vacuum chambers in the South IR experimental section, as measured by cold cathode ion gauges at the center of the section (C00W) and at east- and west-side (C01E and C01W).

Typical RGA spectra in the region clearly indicate desorption of N₂, from the TiN coated surfaces. As shown in Fig. 6, significant high N₂ desorption is related to high-energy photons generated the SCWs in the section. To further demonstrate the point, the ratio of N₂ and H₂ was measured with increasing SCW magnetic field. The results in Fig.7 clearly showed increase of N₂ desorption with SCW SR fan striking the TiN coated surfaces.

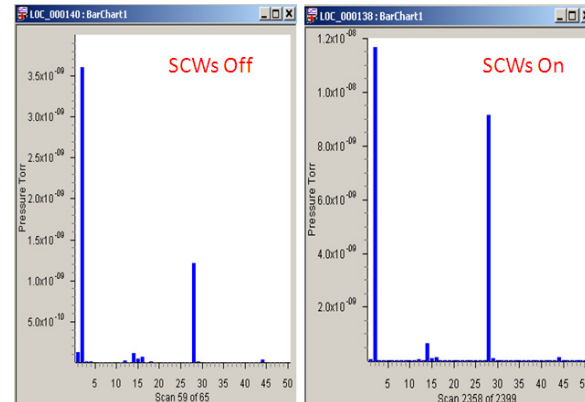


Figure 6: Two typical RGA spectra taken at the center of the South IR, with positron beam energy at 4 GeV.

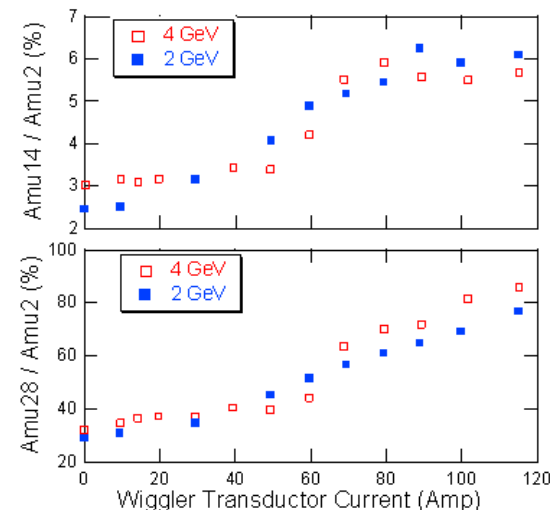


Figure 7: Increased desorption of N₂ from TiN coated surfaces with increasing magnetic field in the SCWs. The measurements were taken with 35 mA positron beam at beam energies of 2 and 4 GeV.

NORTH IR EXPERIMENTAL SECTION

The North Experimental Section (L3) is another long straight, that host (1) SLAC Chicane dipole magnets with RFA on grooved and TiN coated aluminium chambers; (2) RFA equipped quadrupole chamber; (3) NEG coating tests, (4) TE wave measurement, and (5) in-situ SEY measurement system. Fig. 8 depicts the L3 experimental section.

NEG Coating Tests

NEG coating test setup is shown in Fig. 9. To measure effectiveness of NEG coating in EC suppression, a NEG coated stainless steel chamber is equipped with 3 RFAs and a RF-shielded pickup (designed and fabricated by LBNL team). To prevent influences of un-coated beampipes, the test chamber is ‘guarded’ by a pair of NEG coated 1-m long stainless steel beampipes. (The beampipe string was NEG coated by SAES Getters.)

The vacuum performance of the NEG coating was monitored four CCGs and one RGA. After a brief beam conditioning, the NEG coating was activated at 250°C for 24-hour. The beam processing of the NEG coated beampipes is displayed in Fig.10.

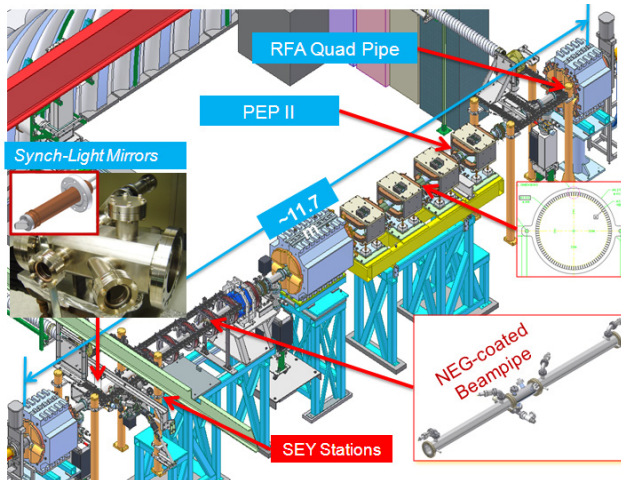


Figure 8. North Experimental Section

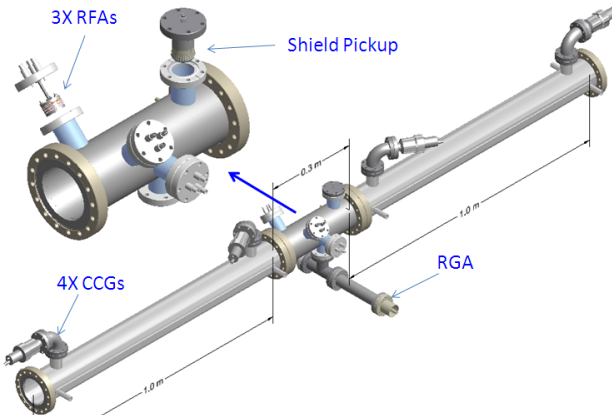


Figure 9. NEG Coating test setup

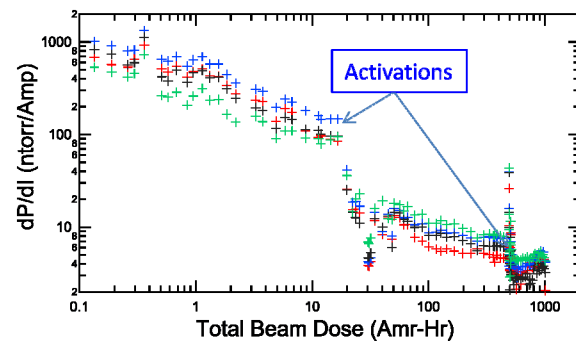


Figure 10. Beam processing of NEG coated beampipes

RFA Quadrupole Chamber

Cornell thin-style RFA was implemented in a bare aluminium quadrupole, as illustrated in Fig.11. The RFA structure consisted of a curved high-transparency Au-plated copper mesh as retarding grid and a flexible circuit detector with 12 segments that provides ~76° coverage. After CesrTA experimental runs from July 2009 to March 2010, the quad RFA beampipe was coated with TiN coating at Cornell. The TiN-coated chamber was re-installed in April 2010 at the same location in L3 for further experiments.

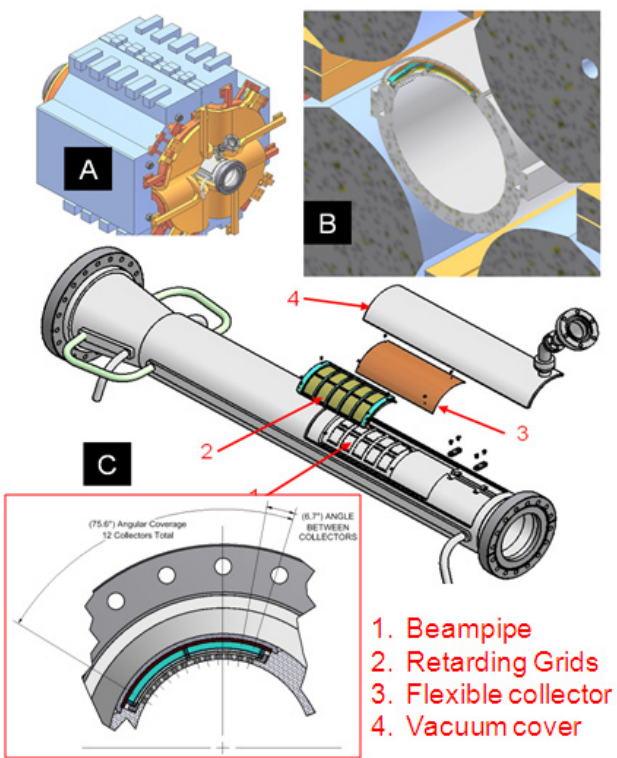


Figure 11. Implementation thin RFA in a quadrupole vacuum chamber

Secondary Emission Yield System

Two SEY systems were installed on a SLAC-build housing chamber. With load-locks, samples of different materials and different coatings can be inserted for SR exposure, without interrupting CESR operations. The

detail description of the *in-situ* SEY system and results are given in this proceeding [8].

SHORT EXPERIMENTAL SECTIONS

Two very short experimental sections (namely Q15W and Q15E sections) were created in the arc of CESR. Each section contains only one bending magnet/chamber and a short straight. With gate valves, many test chambers may be rotated through these sections without significant impact to the CESR operations. So far, many EC-suppression coatings were evaluated on aluminium beampipes. The design of the aluminium beampipe, as shown in Fig 12, incorporated a segmented RFA, two sets of RF-shielded pickups. With this design, bare aluminium, TiN coated and amorphous carbon coated aluminium chambers have been evaluated. The beam conditioning history of these test chambers are summarized in Fig 13, which showed very similar vacuum performances of these surfaces.

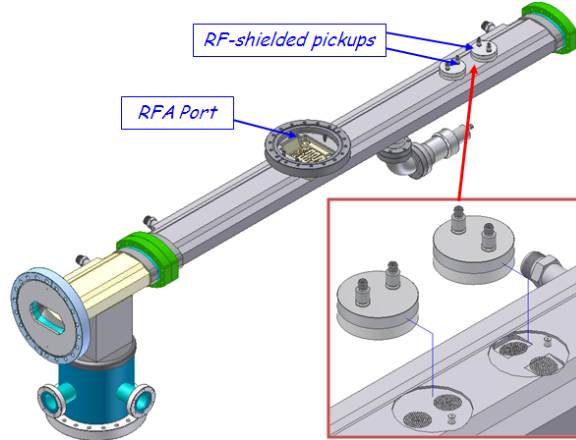


Figure 12. This design of aluminium chamber is used in the short experimental sections at Q15W and Q15E in CESR.

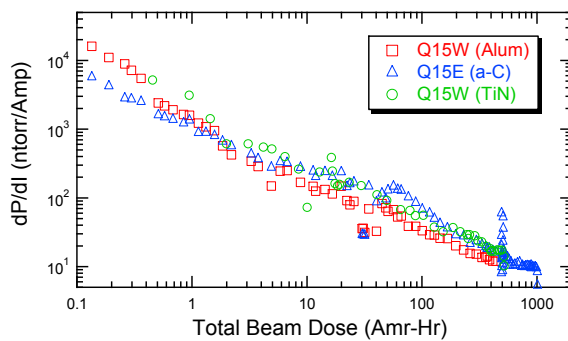


Figure 13. Beam conditioning of bare aluminium, TiN- and amorphous carbon coated aluminium beampipes.

SUMMARY

The reconfigured CESR vacuum system provided flexibility needed for many EC studies for CesarTA. We

have successfully implemented RFAs in all major types magnets (including dipole, quadrupole and wigglers) and drifts. Other EC diagnostics, such as RF-shielded pickups, TE-wave beam buttons, were also deployed in many experimental sections. With these diagnostics, many EC-suppression techniques were evaluated at CesarTA, such as various coatings (TiN, amorphous- and diamond-like carbon, and NEG), grooved surfaces (both triangular and rectangular shaped grooves), and clearing electrode. The vacuum performances of the EC-suppression features were also evaluated.

ACKNOWLEDGEMENT

The Vacuum Group (Brent Johnson, Tobey Moore, William Edward and Brian Kemp) provided excellent technical support throughout the project. It would be impossible to achieve what is described in this paper, without their dedicated assistances.

Ms. Dawn Munson of Lawrence Berkeley National Laboratory (LBNL) and many technical staff member fabricated all the RFA beampipes of the SCWs deployed in the South IR in this study. Their assistances are greatly appreciated.

Dr. Y. Suetsugu of KEK introduced the technique of thermal sprayed EC clearing electrode, and arranged thermal spray of EC clearing electrode for the CesarTA SCW beampipe.

Dr. S. Calatroni and his colleagues at CERN provided assistance in amorphous carbon coating on two Q15 EC-study vacuum chambers.

REFERENCES

- [1] Y. Li, et al, "CESRTA VACUUM SYSTEM MODIFICATIONS" Proceedings of PAC09, Vancouver, BC, Canada, p.357.
- [2] J. Calvey et al, "Electron cloud mitigation investigations at CESRTA", these proceedings.
- [3] D. Rubin, et al, "Overview of the CESR TA R&D Program", these proceedings.
- [4] S. De Santis, et al, "TE wave measurements at CESR TA", these proceedings.
- [5] Y. Li, et al, "Design and Implementation of CesarTA SuperConducting Wiggler Beampipes with Thin Retarding Field Analyzers", Proceedings of PAC09, Vancouver, BC, Canada, p. 3507.
- [6] L. Wang, SLAC, private communications.
- [7] Y. Suetsugu, et al., "Demonstration of electron clearing effect by means of a clearing electrode in high-intensity positron ring". Nucl. Instr & Methods in Phy. Res. Sec. A, 2009. 598(2), p. 372.
- [8] J.S. Kim, et al, "In situ SEY measurements in CesarTA", these proceedings.